FULLY PASSIVE DEGASSING AND FUEL SUPPLY IN DIRECT METHANOL FUEL CELLS

Nils Paust, Christian Litterst, Tobias Metz, Roland Zengerle and Peter Koltay
Laboratory for MEMS Application, Department of Microsystems Engineering (IMTEK),
University of Freiburg, Georges-Koehler-Allee 106, D-79110 Freiburg, Germany

ABSTRACT

In this paper a micro direct methanol fuel cell (µDMFC) is presented, which is operated in a completely passive way, i.e. the cell does not require an external pump for fuel supply. The surface energy of deformed CO_2 bubbles, generated as a reaction product during DMFC operation, is employed to supply methanol to the anode. In contrast to a digital valve based approach presented earlier by Meng et. al. [1], a tapered channel is applied to achieve a pumping mechanism. This way the pump rates can be adapted to the requirements of a specific cell. The presented study reveals that this concept is able to maintain the supply for all typical DMFC operation conditions. Experimental results are presented that demonstrate the continuous operation of a passive µDMFC for more than 15 hours.

1. INTRODUCTION

Miniaturized DMFCs are compact high energy density systems that are easily rechargeable [2]. Therefore, they are promising candidates to compete with Li-Ion batteries in the market of powering small electronic devices**.** Though rapid progress has been made recently, the µDMFC still faces some drawbacks. Amongst methanol crossover [3;4] and a low catalytic activity of the methanol reaction on the anode side [2], the efficient removal of carbon dioxide bubbles is a significant challenge [5]. The bubbles are generated as reaction product on the anode:

$$CH_3OH+H_2O \rightarrow CO_2+6H^+ +6e^- \qquad (1)$$

and may block the active area of the catalyst leading to a performance decrease. Today's common approach to remove CO_2 gas from the anode flow field is to flush bubbles out by an external pump. This results in large complex systems and consumes a significant amount of the produced electrical energy (up to 10%). Therefore, the concept of passively supplied µDMFCs is very attractive [6], especially for small portable appliances. A passive µDMFC, as considered here, operates without the help of external devices for pumping methanol and breathes air on the cathode side. While diffusive supply of air and methanol is quite promising, the removal of carbon dioxide in diffusion driven concepts is mostly based on buoyancy of CO_2 bubbles. For portable devices, this yields significant problems: On the one hand, when scaling down flow field geometries, surface forces become dominant over volume forces which may lead to malfunction of the buoyant bubble removal. On the other hand, the fuel supply is not independent from the orientation of the µDMFC.

The authors have shown earlier that passive CO_2 degassing can be achieved by capillary forces [7;8]. In the present work, the CO_2 bubbles are used to additionally generate a convective flow which pumps the fuel to achieve a fully passive operation. The presented concept for fully passive fluid management in the µDMFC relies again on tapered channels. It is shown that this way a highly flexible passive supply system suitable for all typical DMFC operation conditions can be realized.

2. WORKING PRINCIPLE

Fig. 1 shows a schematic time sequence of a growing bubble from a gas inlet in a liquid filled tapered micro channel with wetting walls (contact angle $\theta < 45°$). As soon as the bubble size reaches the channel height (Fig. 1 at $t = t_1$), the bubble is deformed by the upper and lower channel wall. Different curvatures of the interface at the front and the back of the bubble induce a pressure difference that pushes the bubble in the direction of increasing channel height (Fig. 1 at $t = t_2$).

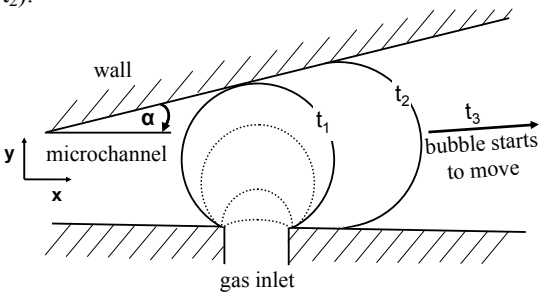

Figure 1: Schematic side view of a time sequence of a growing bubble above an inlet (Ø = 600 µm) in a tapered channel with opening angle α and wetting walls (contact angle $\theta < 45°$).

Before starting to move, the bubbles are kept in place by a pinning force caused by surface roughness and chemical heterogeneities on the channel walls [9]. Depending on the size of the bubble needed to overcome the pinning threshold (Fig. 1 at $t = t_3$), two different pumping modes can be realized: (i) Blocking mode (Fig. 2a) and (ii) non-blocking mode (Fig. 2b). In the blocking mode, apart from corner flow, all liquid displaced by the growing and moving bubbles is directed through an outer loop which means that liquid

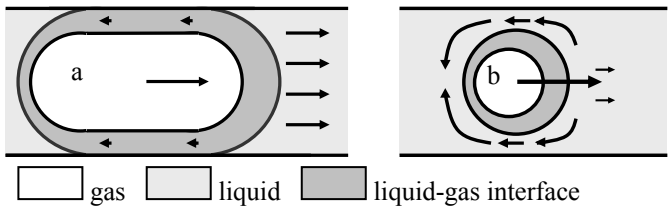

Figure 2: Schematic top view of gas bubbles in tapered channels moving in different pumping modes: a) blocking mode b) non-blocking mode.

is effectively pumped. In the non-blocking mode, the bubble fills only a part of the channel, and the major part of the displaced liquid recirculates directly around the bubble, thus only a small fraction of the displaced liquid contributes to the pumping mechanism.

In the following, the ratio of the liquid flow rate induced by the growing and moving bubble to the generated gas flow rate is referred to as the pumping efficiency (p_{eff}). According to Eq. 1, the molar flow of produced CO_2 is equal to the molar flow of methanol consumed. Thus, the minimum required pump efficiency to sustain the operation of a µDMFC yields:

$$p_{eff} = \frac{\rho_{CO_2}}{M_{CO_2} C_f} \qquad (2)$$

where M_{CO2} is the molecular weight of CO_2, C_f is the molar concentration of the water-methanol solution and ρ_{CO2} is the density of carbon dioxide. The typical concentration for the methanol water mixture feeding the DMFC is situated between 1-4 mol L^{-1}. In the present work, a concentration of 4 mol L^{-1} has been applied. The minimum required pump efficiency is therefore p_{eff} = 1%. In other words: The required methanol supply rate is only about 1% of the generated CO_2 flow rate. In the following, it will be shown that this minimum pump efficiency can easily be achieved by the proposed pumping mechanism.

3. EXPERIMENTAL

For the design process of the passive µDMFC, two different experimental studies were performed: A comprehensive study on the pump performance of moving gas bubbles in single tapered channels and a performance evaluation of a fully passive operating µDMFC.

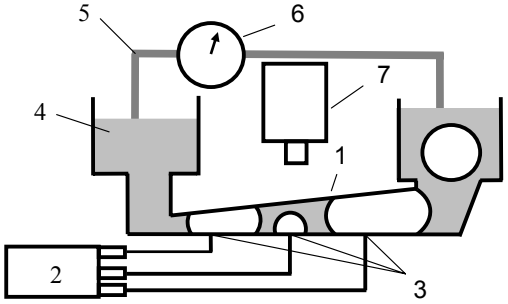

Figure 3: Experimental set-up for the study of the pumping performance of single channels: 1 Tapered channel; 2 Three individual gas inlets: Ø = 0.6 mm; 3 Syringe pump; 4 Reservoir; 5 Silicone tube $Ø_{inner}$= 1mm; 6 Flow sensor; 7 Camera.

Transparent tapered channels

The experimental setup is illustrated in Fig. 3. The transparent fluidic samples were fed externally by a syringe pump through three gas inlets evenly distributed on the channel bottom. In this set-up, the boundary conditions, i.e. gas flow rate and surface properties, were easily adjustable. The applied samples were fabricated by hot embossing in PMMA. The investigated channel geometries were 20 mm long, 3 mm wide and had tapering angles of 1.5° and 3°, respectively. In the experiments, the liquid flow rate was measured by a flow sensor (Sensirion, Type ASL1430-16) as a function of the gas flow rate applied through three syringe pumps (Braun Melsungen).

Fully passive µDMFC

A schematic picture of the considered fully passive µDMFC is depicted in Fig. 4.

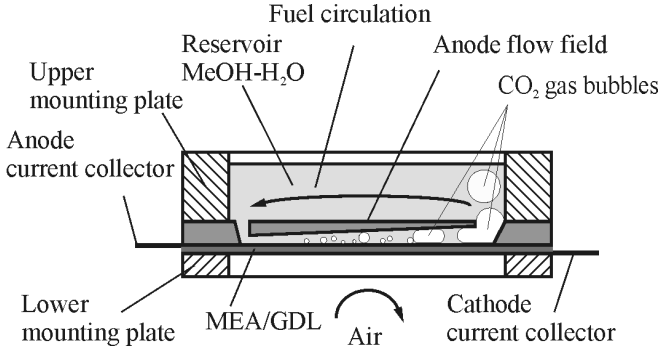

Figure 4: Schematic of a fully passive µDMFC.

Fig. 5 shows an exploded view of the fabricated µDMFC system. The device consists of three cells containing different channel geometries. Each anode flow field comprises three parallel channels that end up in a gas collection channel which is connected with the inlet of the channel through a reservoir to enable fuel circulation. The tapered channel flow fields of the µDMFC were again fabricated by hot embossing in PMMA. Afterwards, collection channels were fabricated by milling with a tapering angle of 10° at both ends of the flow field. The electrical contacts were manufactured by laser cutting of stainless steel (100 µm thickness) and electroplated with a 5 µm gold layer. The sealing consists of casted PDMS. The 100 µm thick MEA (Umicore) had a catalyst loading of 1.5 mg cm^{-2} at the anode side and 1.8 mg cm^{-2} on the cathode side. The active area of a single cell is 3 cm^2.

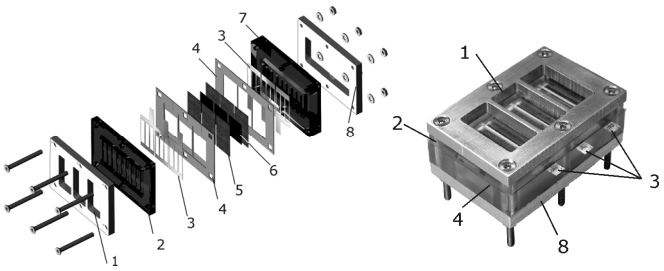

Figure 5: a) Exploded view of the fully passive µDMFC and b) Photograph of the assembled DMFC with the following components: 1 Reservoir; 2 Anode flow field; 3 Electrical contacts; 4 PDMS sealing; 5 Gas diffusion layer; 6 Membrane electrode assembly; 7 Cathode flow field; 8 Lower mounting plate.

The reservoir was filled with a certain amount of a 4 M methanol solution and the fuel cell was operated at its maximum power output under a constant current (20 mA cm^2). During operation the voltage was measured and bubble formation was observed by video recording.

3. RESULTS AND DISCUSSION

Transparent tapered channels

First, the bubble dynamics in the different channel geometries was investigated with respect to the different pumping modes (blocking and non-blocking). Each gas inlet depicted in Fig. 3 was supplied with a gas flow rate of 10 µL min^{-1} and the bubble growth was observed with a camera. The channels walls were coated with a silicate oxide layer in order to obtain hydrophilic channel surfaces. As schematically depicted in Fig 1, the growing and deformed bubbles were kept in place by a pinning force until they reached a certain size and started moving. Table 1 shows the mean size and its standard deviation of gas bubbles detaching from the three gas inlets. At the first two inlets in the 3°-channel, the bubble size of detaching bubbles is below the channel width of 3 mm, therefore, the bubbles start moving without blocking the channel whereas in the 1.5°-channel all moving bubbles do block the channel.

	Alpha = 3° bubble length [mm]	Alpha = 1.5° bubble length [mm]
Inlet 1	2.32 ±0.29	4.08 ±0.21
Inlet 2	2.61 ±0.48	5.31 ±0.25
Inlet 3	4.69 ±0.41	5.97 ±0.48

Table 1: Bubble length of bubbles overcoming the pinning threshold at the three gas inlets of the transparent fluidic channels.

In Fig. 6, the pump efficiency calculated from the applied gas flow rate and the measured liquid flow rate is displayed as a function of the total gas flow rate for different tapering angles of 1.5° and 3°. All measured pump efficiencies were larger than the minimum required value of 1%. The 1.5°-channel shows a 2.3 times larger pump efficiency (up to 13.2%) compared to the 3°-channel (up to 3.8%). This higher efficiency is due to the blocking mode dominating in the 1.5°-channel design whereas the non blocking mode predominates in the 3°-channel and allows for more liquid to bypass the moving bubbles.

Subsequently, surface properties have been modified to adapt to more realistic DMFC operation conditions. One sample was treated as before while another sample was studied untreated ($\theta \sim 35°$). Furthermore, the channel bottom has been covered by a gas diffusion layer (GDL) of 180 µm thickness (SGL, ®SIGRACET GDL31-BA). The results of the pumping efficiencies measured with this setup are depicted in Fig. 7. For the hydrophilic configuration, the channel walls were coated with a silicon oxide layer and also the GDL has been made hydrophilic by plasma activation. It can be seen that in this configuration, the GDL does not significantly influence the pumping performance. The dominating mode is the non-blocking mode. The results are very similar to the ones measured without the GDL plotted in Fig. 6. Due to the complete wetting of the GDL, the bubbles hardly touch the channel bottom. The three phase contact line is very small and pinning effects play a minor role.

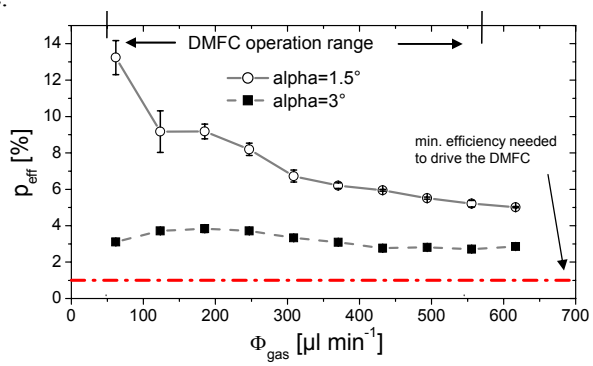

Figure 6: Pumping efficiency p_{eff} plotted against the total gas flow for different tapering angles α.

For the untreated configuration, the three-phase contact angle at the channel walls was about 35°. In this case, the channels operate completely in a blocking mode. The pump efficiency averages to be 1.8 times higher than in the hydrophilic set-up. This higher pump efficiency for the uncoated configuration is a remarkable result for the design of passive flow fields. Though hydrophilization increases the propelling capillary pressure differences over the single bubbles, it does not necessarily lead to an increased pumping performance. In the considered configuration, the higher capillary pressure causes the bubbles to move through the channels without blocking them which results in an even lower p_{eff}. For fuel cell operation, the untreated 3° channel was the most promising geometry and has thus been applied for the µDMFC experiments.

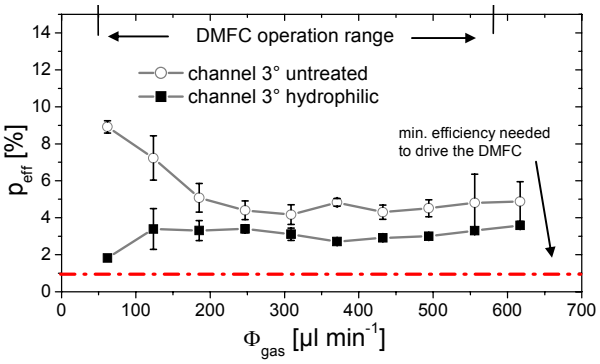

Figure 7: Pumping efficiency p_{eff} plotted against the total gas flow for different surface properties: Opening angle α = 3°.

Fully passive µDMFC

Fig. 8 shows a top view of a 3° tapered channel flow field during µDMFC operation. Now, internally generated CO_2 bubbles moving in the blocking mode supply the fuel cell with methanol. The channel bottom is covered by a GDL as in the experiments with the previously studied untreated 3°-channel. In Fig. 8, the menisci of the back of the bubbles are clearly flattened indicating that contact line pinning has a significant influence leading to the blocking pumping mode. The power performance of long term experiments at a constant current of 20 mA cm^{-2} is depicted in Fig. 9. The electrical power output, as determined from the measured current and voltage, is displayed as a function of time. It can be seen that the runtime

of the cell before it stops operation due to starving is proportional to the filling volume of the reservoir. A total filling volume of 3.2 mL (4 M MeOH) leads to a power breakdown after about 4 hours continuous operation, while a filling of 9.2 mL enables a continuous runtime of more than 15 hours. This indicates that the cell operates until all methanol initially supplied to the reservoir has been consumed completely. The fuel cell operates passively at ambient temperature and pressure with no external actuation or support of any kind. Recharging was possible by simply refilling the reservoir.

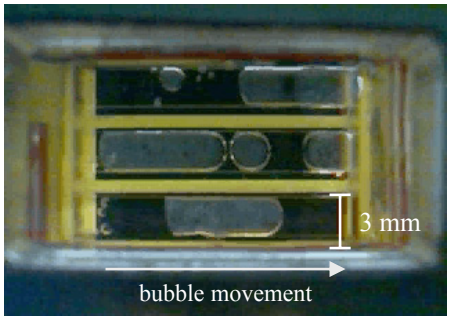

Figure 8: Photograph of the flow field with CO_2 bubbles in the blocking mode during fully passive operation.

For the ultimate verification of fuel circulation in the µDMFC, the reservoir has been divided in half and the inlet and outlet of the channels were connected via a flow sensor similar to the setup shown in Fig. 3. At a constant current of 20 mA cm^{-2} corresponding to a theoretical gas flow rate of 51 µL min^{-1} in each channel, the liquid flow rate was measured to be approximately 5 µL min^{-1} per channel. This corresponds to a pumping efficiency of 9.8% which is in good agreement (p_{eff} = 9% at Φ_{gas} = 62 µL min^{-1}) with the experimental results in the single channels externally fed by the syringe pumps.

4. CONCLUSIONS

A fully passive supply method for µDMFC systems has been proposed and experimentally characterized. The working principle based on capillary forces does not require any external actuation or support to supply the fuel cell with methanol. Furthermore, CO_2 bubbles are safely removed by capillary forces through the tapered channel design. The experiments indicate that the runtime of a µDMFC operated with this method is proportional to the amount of methanol initially supplied and power production is sustained as long as fuel is available in the reservoir. The maximum runtime of such a passive µDMFC observed by experiments was more than 15 hours with a loading of 9.2 mL 4 M methanol-solution. In all studied configurations, the pump efficiencies were large enough to enable a continuous µDMFC operation which requires a pump efficiency of at least 1% for a 4M Methanol solution. The highest pump efficiency observed with this approach was 13.2%. The pump efficiencies can be adapted to specific requirements and operating conditions by changing the channel design and the surface properties of the channel walls. Therefore, the pumping mechanism can be considered as a highly flexible and robust supply mechanism that is suitable for a broad range of µDMFC applications.

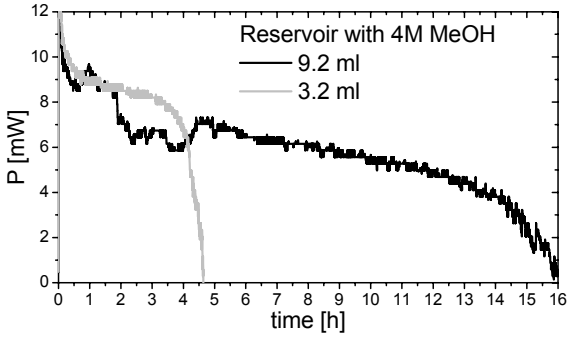

Figure 9: Power performance of the fully passive µDMFC for different reservoir fillings.

5 Acknowledgements

This work was supported by the German Ministry of Science and Education within Project 03SF0311B, the German Federal Ministry of Economics and Labour (BMWA) within the VDI/VDE InnoNet-program PlanarFC and the German Research Council within Project 527/3.

References

[1] D. D. Meng and C.-J. Kim, "Embedded self-circulation of liquid fuel for a micro direct methanol fuel cell," in *Proc. of IEEE MEMS 2007,* Kobe 2007, pp. 85-88.

[2] Dillon R. et al.: "International activities in DMFC R&D: Status of technologies and potential applications," in *Journal of Power Sources*, Vol. 127, No. 1-2, pp. 112-126, 2004.

[3] Ma Z.Q. et al.: "A palladium-alloy deposited Nafion membrane for direct methanol fuel cells," in *Journal of Membrane Science*, Vol. 215, No. (1-2), pp. 327-336, 2003.

[4] B. K. Kho et al.: "On the consequences of methanol crossover in passive air-breathing direct methanol fuel cells," in *Journal of Power Sources*, Vol. 142, No. 1-2, , pp. 50-55, 2005.

[5] R. Chen et al.: "Effect of cell orientation on the performance of passive direct methanol fuel cells." *Journal of Power Sources*, Vol. 157, No. 1 , pp. 351-357, 2006.

[6] T. Shimizu et al.: "Design and fabrication of pumpless small direct methanol fuel cells for portable applications. *Journal of Power Sources*, Vol. 137, No. 2, pp. 277-283, 2004.

[7] C. Litterst, S. Eccarius, C. Hebling, R. Zengerle, and P. Koltay, "Novel Structure for Passive CO2 Degassing in µDMFC," in *Proc. of IEEE MEMS 2006*, Istanbul 2007, pp. 102-105.

[8] C. Litterst et al.: "Increasing µDMFC efficiency by passive CO_2 bubble removal and discontinuous operation," in *Journal of Micromechanics and Microengineering*, Vol. 16, No. 9, p. S248-S253, 2006.

[9] L. C. Gao et al.: "Contact angle hysteresis explained," in *Langmuir*, Vol. 22, No. 14 , pp. 6234-6237, 2006.